

Main components of full-waveform inversion for reservoir characterization

Ehsan Zabihi Naeini^{1*}, Tariq Alkhalifah², Ilya Tsvankin³, Nishant Kamath³ and Jiubing Cheng⁴

Abstract

Building a 3D reservoir model, which has become a key part of reservoir management, is a challenging task. Classic seismic inversion techniques, both deterministic and stochastic, have attempted to reduce the uncertainty in reservoir modelling. However, these inversion methods are typically based just on amplitude and make a number of critical simplifying assumptions, such as that migrated data are accurate and can be modelled by 1D convolution (using reflection coefficients computed from the Zoeppritz equation or its linear approximations). Migration algorithms themselves may suffer from inadequate amplitude and multiple-scattering treatments. Full-waveform inversion (FWI), specifically designed for the direct estimation of the reservoir parameters, is proposed here as an alternative method for seismic reservoir characterization. This is clearly an ambitious goal, and it is not our intention to claim we have already achieved it. Instead, we intend to introduce the main components of such reservoir-oriented inversion and discuss a strategy for elastic, anisotropic FWI constrained by rock-physics models and facies types. Among the many challenges, we focus mostly on understanding the physics and describing some elements of an efficient forward-modelling engine. In particular, we show how analysing the radiation patterns helps to optimise the parameterisation and could reduce the null space.

Introduction

A reservoir in the geoscience sense describes a natural storage unit of fluids or gas inside the Earth. The reservoirs usually contain brine, oil, or gas, two of which are the main objective of oil and gas geophysical (and specifically seismic) exploration. Such reservoirs commonly reside at depths between 2 and 5 km, with the lateral extent on the order of tens of kilometres and thickness that does not usually exceed 300 m (one could argue a net pay above 50 m is a better than average reservoir). A 3D reservoir model has become a key part of reservoir management. Building such a model is, however, a challenging task. It should be ‘simple’ as well as ‘complex’, ‘simple’ (or fit-for-purpose) so it contains basic features that have a real impact on field production (e.g., faults) and ‘complex’ so that it can explain the structural and heterogeneous makeup of the reservoir. Therefore, a major challenge is how to provide a close integration between the seismic discipline (e.g., complexities involved in the inversion of seismic data) on one hand and reservoir modelling (e.g., simplicity required to match the production) on the other. This is often known as ‘closing the loop’ concept, which has also led to innovative techniques such as stochastic or geostatistical inversion (Psaila, 2011).

Seismic inversion, in principle, provides information about the spatial distribution of elastic parameters between

the wells, which can then be converted into reservoir properties (e.g., porosity and saturation) using petro-elastic models. However, seismic sections have a limited vertical resolution compared to the scale of the reservoir model. Full field reservoir models are often generated in cellular format, in which each cell may be 100 m by 100 m horizontally and on the order of 1 m vertically. Seismic data, however, typically have higher resolution laterally than vertically when compared with the reservoir model standards (e.g., about 25 m by 25 m laterally and 10 m vertically). In addition, the seismic inversion process is non-unique, like many other geophysical inversion problems.

Nonetheless, the current reservoir characterization workflows are based on ‘classic’ seismic inversion techniques. By ‘classic’ we mean all techniques that make use of the amplitude variation of seismic data with offset or angle (AVO/AVA) to invert for elastic or reservoir properties in deterministic or stochastic fashion (Russell, 1988; Coléou et al., 2005). These techniques have generally served us well but maybe it is time to think of better ways to characterize reservoirs. There is no doubt that the main driver is *the hope* for more accurate results, especially at this time of industry downturn with high demand on less cost and more efficiency. Breaking the old tradition is, however, not easy and the only chance to do so may well be with FWI considering the

¹ Ikon Science.

² King Abdullah University of Science and Technology (KAUST).

³ Center for Wave Phenomena, Colorado School of Mines.

⁴ Tongji University.

* Corresponding author, E-mail: enaeini@ikonscience.com

excitement and the promise it has brought to our industry recently. Whether it comes with less cost is yet to be determined. We would like to emphasize the fact that there are good features in the classic methods that we have learnt over the past couple of decades and can still benefit from. This will be discussed later.

The classics

The concept of closing the loop mentioned above is aiming to address two issues with classic seismic inversion: vertical resolution and non-uniqueness. Coléou et al. (2005) proposed one such approach that is schematically displayed in Figure 1. The key feature of their work is that the initial reservoir model (and also the updates) is defined on a fine-scale stratigraphic grid in depth. The petro-elastic model (PEM) specified by the user transforms the reservoir model into elastic properties so that synthetic gathers can be computed using the Zoeppritz equation (or its linear approximations) and compared with the real seismic data. If the difference exceeds a certain threshold, the updates are applied and this loop is repeated until convergence. After convergence, the final reservoir model honours the seismic *amplitudes* (note it is only amplitudes but not waveforms) and is consistent with the specified PEM. The time-to-depth consistency is also guaranteed through the inverted velocity model.

Saussus and Sams (2012) further argue that a key component of any such procedure should be facies. Perhaps the most straightforward reason for this is that geologists might use the shape, distribution, size and multiple nested

scales of different facies to assess the plausibility of the reservoir model. Although facies could be computed using the seismic data directly (for example from inverted elastic properties), it is not desirable to do so owing to the limited vertical resolution, which would result in the output facies being too smooth (potentially averaging out any small-scale facies variations). This again demonstrates why facies should be part of the ‘closing the loop’ workflow shown in Figure 2. When compared with Figure 1, one can note that the petro-elastic models are also defined in terms of facies, which in turn further constrains the inversion and guides it towards a unique reservoir model.

One should note that constraining seismic inversion to obtain geologically plausible (and mathematically unique) elastic models has also been implemented in deterministic-type algorithms (Russell, 1988). These types of constraints are often included in the form of a linear relationship between elastic properties (e.g., acoustic impedance and density). This approach, however, inevitably imposes the same linear trend for all facies in the model, which can be easily violated because this trend might be different, for example, in shales and sands. To address this issue, Kemper and Gunning (2014) developed a joint impedance and facies inversion using a Bayesian framework to allow for a different rock-physics model for each facies type.

What we have just described summarizes much of the seismic industry’s efforts from 1980s to date to address accuracy and resolution challenges in reservoir characterization. Let us finish this section with a quick review of the shortcomings and good lessons learnt from the classic methods. General shortcomings: they are (a) post-migration, (b) based on the 1D convolutional model, and (c) use only amplitude information (not waveforms). Good lessons: (a) the ability to use rock physics, (b) inversion for facies and application of rock-physics relations per facies, and (c) they achieve acceptable resolution in the depth domain (the ultimate goal of accurate reservoir models).

FWI: the new trend

FWI has emerged recently as a powerful tool for seismic velocity model building, which provides the input for migration algorithms and ultimately results in a better structural image. This is despite its huge cost and many simplifying assumptions. One can intuitively understand that such improvement is because of the higher resolution and, therefore, superior quality of FWI-based velocity models. It is this improved resolution and accuracy potential of FWI that gives us the hope to push FWI applications beyond imaging and utilize it to characterize the reservoir. The very first attempt to achieve this would be to estimate elastic properties (e.g., acoustic impedance, shear impedance, and density) using FWI. This is also known as elastic FWI, whose schematic workflow is shown in Figure 3 (an example of elastic FWI is shown in Guasch et al., 2012). One could argue that such an advance would replace the current practice of quantitative

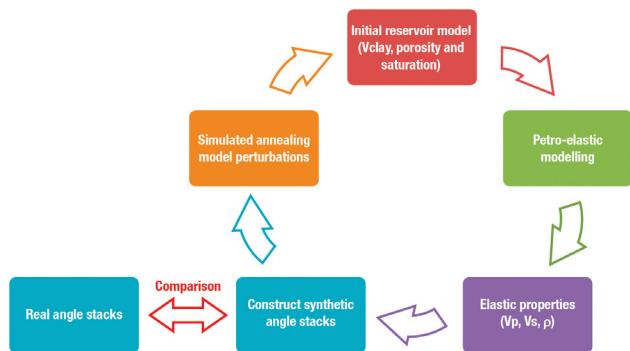


Figure 1 Petrophysical seismic inversion workflow adapted from Coléou et al. (2005).

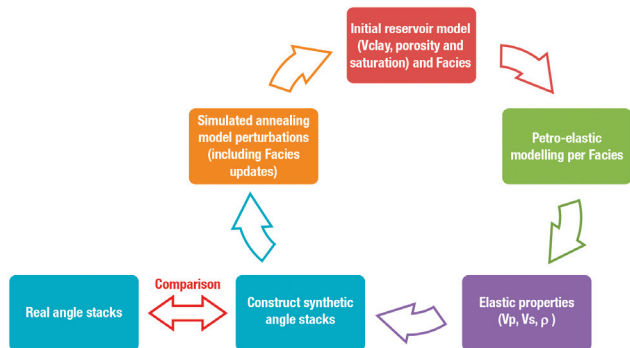


Figure 2 Stochastic inversion workflow adapted from Saussus and Sams (2012).

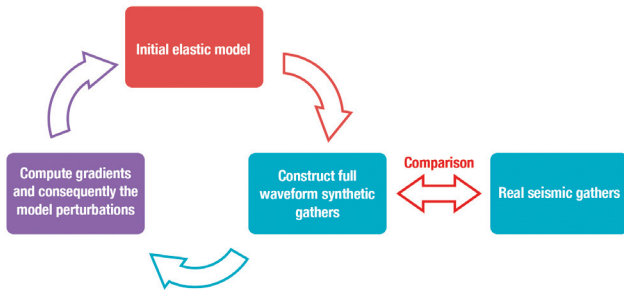


Figure 3 Schematic workflow for elastic FWI.

interpretation for estimating the elastic properties using classic AVO-based inversion (Russel, 1988).

The beauty of FWI, given that we can get the physics right, is that it will appropriately address the shortcomings of the classic methods mentioned in the previous section. Indeed, FWI employs waveforms, is not based on convolutional model assumption, and involves no ambiguity in the treatment of amplitudes and multiple scattering during migration. In fact, there is no longer a need for a separate migration step as it becomes part of the FWI process. However, we must incorporate the good lessons as well to replace the classics (compare Figure 3 with Figures 1 and 2). This leads us to propose the following considerations for any FWI-based reservoir-characterization applications.

Rock-physics constraints: It is common practice to have some rock-physics constraints, even in basic deterministic AVO-type inversions, to ensure a geologically plausible model. Their inclusion in the FWI engines is therefore strongly desired.

Facies: It is essential to incorporate those into the inversion so that the obtained model gives the correct facies distribution. It is also important to have rock-physics models defined for each individual facies at an appropriate scale. This could potentially help to better constrain the anisotropy parameters of each facies, as will be discussed shortly.

Closing the loop: to address the need for higher resolution in depth and invert directly for reservoir properties.

We shall push the FWI-based approach even further by taking into account both intrinsic and fracture-related anisotropy. As an example, let us consider Ghawar field in Saudi Arabia, the biggest oil field on Earth. It produces about 5 million barrels a day, half the Saudi production. An enhanced understanding of the fracture network over this large field including estimates of the fracture density and orientation can help in developing strategies for improved oil recovery through better drilling and injection decisions. Roughly speaking, only a 1% increase in oil recovery in Ghawar is equivalent to the production of Saudi Arabia for a year. Analysing the anisotropic signatures of seismic data acquired over such fields (other examples exist around the world, and some of these fields are in decline) can reveal the fracture systems and optimize production of hydrocarbons (Tsvankin and Grechka, 2011). Hence, we believe anisotropy, along with elasticity, should be considered in any new FWI-based reservoir characterization method.

Progressively, one can start with an FWI engine such as the one in Figure 3 and then proceed towards the more advanced anisotropic- and facies-based workflow schematically depicted in Figure 4. Nonetheless, it is important that the main components of FWI are recognised, and we shall discuss them in the following sections. One could also add attenuation to this workflow but it is beyond the scope of this paper.

Despite the simplistic look of Figure 4, it includes very complex mathematical, geophysical, geological, engineering, and computational challenges. Some of the current industry gaps such as the ones between the reservoir engineer and geophysicist or between the geophysicist and geologist must be closed. If we believe that FWI captures the physics correctly, then we cannot accept a scenario where the reservoir model produces a good history match but does not match the seismic data. On the other hand, the fact that all the authors of this paper are geophysicists indicates how much work is still required to build up an effective multi-disciplinary collaboration in reservoir characterization (we hope the interested readers will join us to achieve this goal).

FWI – The main components

The main components of FWI for seismic reservoir characterization can be summarised as follows: *the reservoir model, the physics, forward modelling, and an inversion engine.* These components are interlinked. For instance, the desired reservoir model drives the physics which then subsequently governs the development of forward modelling. One could argue that devising a physically adequate and efficient forward modelling algorithm is the main bottleneck for FWI to become the standard practice for reservoir characterization. For example, the finite-difference (FD) method which is commonly used for wavefield extrapolation, is strongly affected by numerical dispersion as the frequency bandwidth increases, forcing us to use finer-sampled grids, which subsequently increases the computational cost. The cost becomes *prohibitively* high for anisotropic and elastic wave modelling owing to the spatial variations of the velocity field. For this reason, high-resolution FWI is still a challenge that limits the potential applicability of our approach for reservoir characterization. Numerous parameters and their coupling (trade-offs) cause other difficulties which will be discussed later.

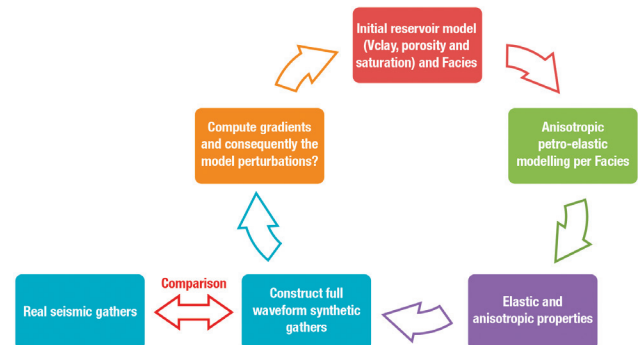


Figure 4 Schematic workflow for anisotropic elastic reservoir-oriented FWI.

Here, we first briefly describe the main components of FWI and then we focus on two of those components: the physics and forward modelling. We reiterate that it is not our intention to claim we have thoroughly researched all these components and solved the problem. Instead, we intend to express our ideas, review some of our results and outline our plans for future work, in part to stimulate other researchers.

Reservoir model

The model consists of reservoir properties in depth with a desired vertical resolution in the order of several metres. As mentioned, reservoir properties are linked to elastic properties (and, therefore, seismic data) via petro-elastic relationships. It is yet to be examined whether one can directly compute the FWI updates as a function of reservoir properties (note the question mark in the orange box in Figure 4). Other potentially challenging factors that one has to handle include the incorporation of the over/under burden. That is because the reservoir engineer is only interested in the reservoir region while FWI estimates the reservoir properties using waves propagating through the entire section. One idea to explore is to focus the FWI updates only in the reservoir region after fixing the kinematics of wave propagation through the over/under burden. Another possibility is to formulate FWI such that it simultaneously updates the kinematics in the over/under burden (e.g., parameters affecting the propagation only) and the reservoir properties in the target region. This approach is supported by our initial analysis of the scattering potential of some of the reservoir properties, sensitivity study of the wave-propagation parameters and an innovative representation of the model space.

Physics

Most current FWI algorithms are acoustic and focus on inverting diving (or also known as transmitted) waves. Acoustic models, however, are inadequate for the purpose of seismic reservoir characterization because they do not produce the correct P-wave reflection coefficient and do not include shear-wave velocities. Accurately defining the physics needed to simulate seismic data is crucial to our implementation of FWI.

The presence of aligned fractures and non-hydrostatic stresses makes most reservoir formations azimuthally anisotropic. In some cases, the reservoir matrix itself is intrinsically anisotropic – in particular, shales are always transversely isotropic (TI) with the symmetry axis usually orthogonal to layering. The simplest azimuthally anisotropic model is TI with a horizontal symmetry axis (HTI), but it describes only a single set of parallel, penny-shaped cracks embedded in a purely isotropic background matrix. A much more realistic model is orthorhombic, which typically remains adequate for multiple vertical fracture sets embedded in a VTI (TI with a vertical symmetry axis) background (Grechka and Kachanov, 2006; Tsvankin and Grechka, 2011). Hence, our strategy

would be to treat the reservoir volume (but not necessarily the over/under burden) as orthorhombic in the modelling and FWI algorithms.

Within the seismic frequency range (e.g., from 2 to 80 Hz), such elastic anisotropic formulation should explain many of the phase and amplitude features of observed waveforms. Kamath and Tsvankin (2013) show that taking into account both anisotropy and elasticity in FWI of reflection data from layer-cake VTI media helps to obtain the interval medium parameters that cannot be otherwise constrained by acoustic algorithms. This indicates that, by successfully implementing the orthorhombic model in FWI, we can possibly get one step (and that is a big step!) closer to producing high-resolution estimates of the reservoir parameters.

It is, however, critically important in the inversion process to find the optimum set of reservoir parameters that can explain (and be constrained by) our data. This requirement addresses a big problem in multi-parameter FWI, the null space (i.e., the trade-offs between the parameters; see Operto et al., 2013; Alkhalifah and Plessix, 2014). Trade-offs are often addressed by applying user-defined regularization (e.g., here is where rock-physics relationships can be used). The impact of such constraints should be carefully weighted to avoid suppressing the impact of the data. For interpretation purposes, however, we need to know the physical meaning of the chosen medium parameters and their relationship with the reservoir properties, such as saturation, porosity, facies etc.

To optimize the parameterization, we perform sensitivity analysis by examining the radiation patterns (e.g., Alkhalifah and Plessix, 2014), which relate changes in the wavefield (as a function of angle of incidence) to perturbations in model parameters. As will be discussed below, this provides valuable insight into parameter trade-offs and should help in designing an effective FWI algorithm.

Modelling

Modelling is an essential part of FWI. In fact, modelling and the physical assumption of the medium go hand-in-hand. Apart from numerical dispersion at higher frequencies, which hampers the FD modelling, elastic FWI also remains exposed to a range of complexities induced by multi-component data, such as multi-mode coupling and conversions of seismic waves (i.e., several parameters may have a similar effect on the seismic response for a particular propagation regime, from transmission to reflection). Wave-mode decoupling, which is already an essential part of elastic imaging (Dellinger and Etgen, 1990; Yan and Sava, 2008) has become a new strategy to reduce parameter trade-offs in FWI (Wang and Cheng, 2015). Thus, we plan to develop a new efficient spectral-based modelling engine for elastic FWI that can simultaneously propagate the decoupled wave modes and the total wavefields. This is further discussed below. Also, we plan to investigate other recent developments in modelling algorithms for orthorhombic media (Fowler and Lapilli, 2012; Song and Alkhalifah, 2013).

Full-waveform inversion

After defining our reservoir model representation and the modelling engine supported by the correct physics, we have to find an efficient way to actually invert the data (ideally in a ‘close the loop’ fashion). That means we should think about optimizing the implementation, especially the model-updating process, and also consider parameter trade-offs and regularization to ensure successful convergence. Recently developed objective functions and gradient-conditioning approaches can be used to improve the convergence of the inversion algorithm. The focus on the reservoir is meant to make the targeted 3D implementation practical. Our future research will include finding the proper objective function, computing the FWI gradient directly as a function of reservoir parameters, and conditioning of the gradient to achieve a successful inversion (an example is in Alkhalifah, 2015).

Radiation patterns (towards understanding the physics)

FWI process is basically designed to predict the scattering potential of the model in an iterative fashion. Transforming the residuals into the updates in the velocity model (this process is at the heart of FWI) can be based on a linearized form of the wave equation referred to as the Born approximation (Cohen and Bleistein, 1977; Panning et al., 2009). In inverting for multiple parameters (e.g., for anisotropic media), we construct formulas that relate the residuals to perturbations in each parameter, which allows for updates in these parameters in the process of fitting the data (whether or not we can implement the idealised flow in Figure 4 and directly update the reservoir parameters is the subject of future research). It is paramount, though, to mitigate the trade-offs and focus on the parameters we *can* obtain from seismic waveforms considering the coverage and make-up of the input data (e.g., bandwidth, offset range, azimuthal coverage, etc.).

Parameterization is of particular importance in devising any processing or inversion algorithm for anisotropic media. The widely used notation for TI media suggested by Thomsen (1986) includes the vertical velocities of P- and S-waves (V_{p0} and V_{s0}) and the anisotropy coefficients ϵ , δ , and γ . Thomsen parameters not only simplify the description of seismic signatures, they reduce trade-offs in building TI models from seismic data. In particular, P-wave kinematics, known to be controlled by four stiffness coefficients, depends on just three Thomsen parameters (V_{p0} , ϵ , and δ), with δ primarily responsible for the velocity near the symmetry axis (and, therefore, for small-offset reflection traveltimes in VTI media). This and many other advantages of Thomsen notation are valid for TI models with any strength of velocity anisotropy, as discussed in detail by Tsvankin (2012).

Such reduction in the number of independent unknowns is exactly what we are looking for to mitigate trade-offs in FWI. Indeed, most acoustic FWI algorithms for TI media operate with V_{p0} , ϵ , and δ or their combinations, such as the anellipticity coefficient η [$\eta \equiv (\epsilon - \delta) / (1 + 2\delta)$], which is the

only anisotropy parameter needed for P-wave time processing in VTI media (Alkhalifah and Tsvankin, 1995).

Most benefits of Thomsen parameters can be preserved for orthorhombic media by employing the notation introduced by Tsvankin (1997, 2012), which also captures the combinations of the stiffnesses constrained by seismic data. For a known orientation of the three mutually orthogonal symmetry planes (one of which is assumed to be horizontal), the orthorhombic model is described by the vertical velocities of the P-wave and the S-wave polarised in the x_1 -direction (V_{p0} and V_{s0}) and seven anisotropy coefficients. Two sets of Thomsen-style anisotropy parameters are defined in the vertical symmetry planes $[x_2, x_3]$ ($\epsilon^{(1)}, \delta^{(1)}, \gamma^{(1)}$), and $[x_1, x_3]$ ($\epsilon^{(2)}, \delta^{(2)}, \gamma^{(2)}$) and one more coefficient ($\delta^{(3)}$) in the horizontal symmetry plane (Figure 5, the superscript refers to the axis orthogonal to the corresponding plane). P-wave kinematics even in strongly anisotropic orthorhombic media is governed by just six parameters out of nine -- V_{p0} , $\epsilon^{(1,2)}$, and $\delta^{(1,2,3)}$. This notation also ensures a seamless transition between different anisotropic models in inversion algorithms because both VTI and HTI media represent special cases of the orthorhombic model and are described by subsets of Tsvankin’s parameters. Note that if reservoir rocks are intrinsically isotropic (e.g., sandstones or carbonates), multiple vertical fracture sets produce an effective medium described by a special type of orthorhombic symmetry defined by just six independent parameters (Grechka and Kachanov, 2006; Tsvankin and Grechka, 2011).

In general, inversion for orthorhombic media involves 12 unknowns – nine parameters introduced above and three Euler angles that define the symmetry-plane orientation. These 12 parameters may vary vertically or laterally and, ideally, we should invert for them in every cell of the model. Even for multi-component and multi-azimuth surface seismic recording, usually we can only invert for some of these

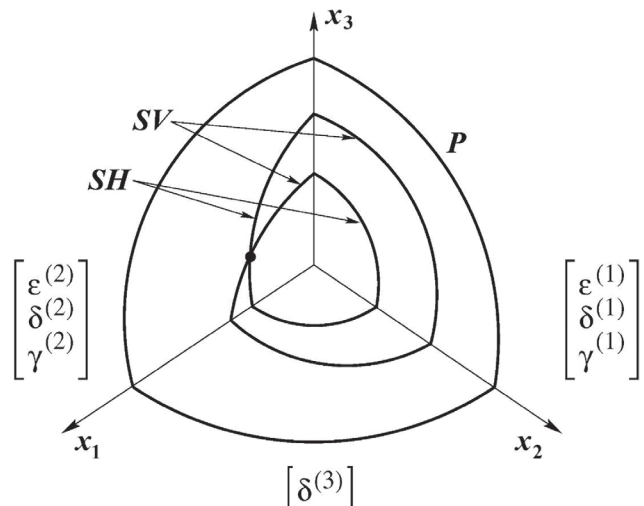


Figure 5 Cartoon of phase-velocity surfaces and notation for orthorhombic media (after Tsvankin and Grechka, 2011). The co-ordinate planes coincide with the symmetry planes of the model. The fast S-wave represents an SH mode in the $[X1, X3]$ -plane and SV mode in the $[X2, X3]$ -plane; for the slow S-wave, the opposite is true.

parameters (or their combinations), so it is essential to know what trade-offs we may encounter in the inversion.

Interestingly, the fact that we include facies in FWI (see Figure 4) helps us to enforce an appropriate anisotropic definition for each facies. For example, if the overburden facies is shale then TI parameterization should be suitable (if the shale is not fractured) and if the reservoir is composed of fractured carbonates, then that could require orthorhombic definition. In principle, this should lead to a better parameterization of the reservoir model and optimization of the inversion.

Since our focus is on the reservoir, we need to evaluate the high-resolution components of these parameters, which are described by their scattering potential. Using perturbation theory, we perform sensitivity analysis by employing plane-wave decomposition of the Born scattering expressions with respect to parameter perturbations. The resulting radiation patterns, which relate the perturbations in the medium parameters to the data, allow us to reveal parameter trade-offs and, potentially, identify parts of the data needed to constrain a given parameter. In simpler terms, we should look out for parameters with similar radiation patterns (i.e., simultaneously inverting for those parameters will not be realistic) or for parameters with radiation patterns that differ only at large angles (i.e., indicating that long offsets are required for a successful inversion).

Below we analyse radiation patterns for acoustic and elastic TI and then elastic orthorhombic media. This transition helps one to better understand the associated complexities as they increase from one model to the next.

Acoustic TI media

Acoustic TI media can be described by a velocity parameter and two anisotropy coefficients. For the former one could use the P-wave vertical velocity (V_{p0}), horizontal velocity (V_{hor}) or normal-moveout (NMO) velocity for horizontal reflectors (V_{nmo}). The latter two are related to V_{p0} through Thomsen parameters, i.e., $V_{hor} = V_{p0}\sqrt{1+2\epsilon}$ and $V_{nmo} = V_{p0}\sqrt{1+2\delta}$. Here, we rely on a parameterization for the acoustic VTI model that includes V_{nmo} , δ , and the anellipticity coefficient η . The advantages of using other parameter combinations, for example, $(V_{p0}, \epsilon, \delta)$, (V_{nmo}, η, δ) , and $(V_{hor}, \epsilon, \eta)$ were discussed by Shen (2012), Gholami et al. (2013), Alkhalifah and Plessix (2014) and Alkhalifah (2015). The velocity in each of those parameterizations has a purely 'isotropic' radiation pattern (i.e., similar to that of V_{nmo} in Figure 6). While this would result in a wide range (low to high) of wavenumber updates in the velocity, there will inevitably be trade-offs between the velocity and anisotropy parameters. For example, in Figure 6 there is a trade-off between V_{nmo} and δ for small opening angles, and between V_{nmo} and η for opening angles close to 180° . The radiation patterns in Figure 6 also demonstrate that larger offsets are needed to update η pointing to the need for diving waves. This simple experiment already gives us an indication of what challenges we might encounter in the more complex orthorhombic media.

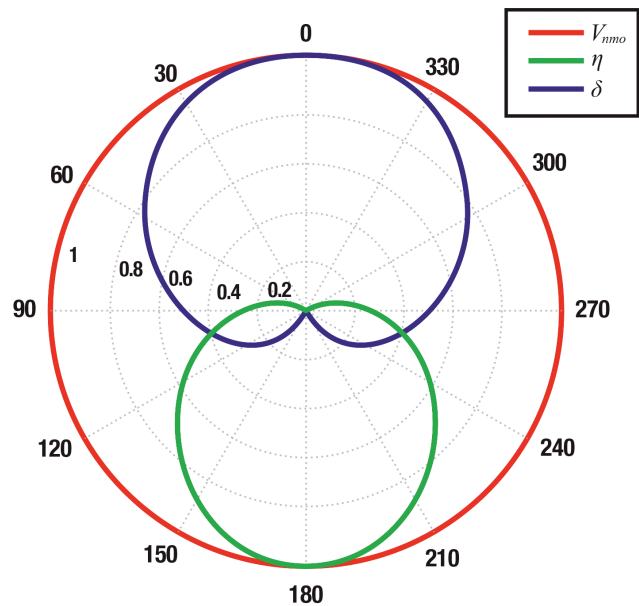


Figure 6 Radiation patterns of P-wave scattering in acoustic VTI media for perturbations in V_{nmo} , δ , and η . This plot is in terms of opening angles and the radius shows the radiation scattering magnitude.

Elastic TI media

Next, we consider an elastic, homogeneous, isotropic background medium with spatially varying perturbations in the stiffness coefficients. Assuming the background to be isotropic and homogeneous allows us to obtain relatively simple expressions for the radiation patterns. As discussed above, we first represent the elastic wave equation, which includes a perturbation in the stiffness tensor as the source, in the Born approximation (Calvet et al., 2006; Alkhalifah and Plessix, 2014). The solution of the wave equation, which yields the perturbed (scattered) wavefield, is expressed in terms of the asymptotic Green's functions (Vavryčuk, 2007). Once the radiation patterns for perturbations in the stiffness coefficients have been obtained, the chain rule is employed to derive the patterns for the desired model parameterization.

The radiation patterns of the transmitted P- and SV-waves for perturbations in the velocities V_{p0} , V_{s0} , V_{nmo} , and V_{hor} (other parameterizations are subject of further research) are plotted in Figure 7. Not surprisingly, the transmitted P-wave is not sensitive to the shear-wave velocity V_{s0} . However, the transmitted SV-wave is sensitive (in addition to V_{s0}) to the velocities V_{nmo} and V_{hor} (Figure 7b), which can help to constrain these parameters if multi-component data are available. A perturbation in the velocity V_{s0} scatters the SV-wavefield uniformly for the entire range of incidence angles (Figure 7b), likely owing to the fact that V_{s0} also represents the horizontal SV-wave velocity. The SV-wave radiation patterns of V_{nmo} and V_{hor} are similar to that of V_{nmo} for the P-wave (Figure 7a).

For the P-wave reflected from a horizontal interface, the radiation patterns for V_{p0} , V_{nmo} , and V_{hor} (Figure 8a) are the same as those for the transmitted P-wave (Figure 7a). The difference, however, is that the reflected P-wave in the

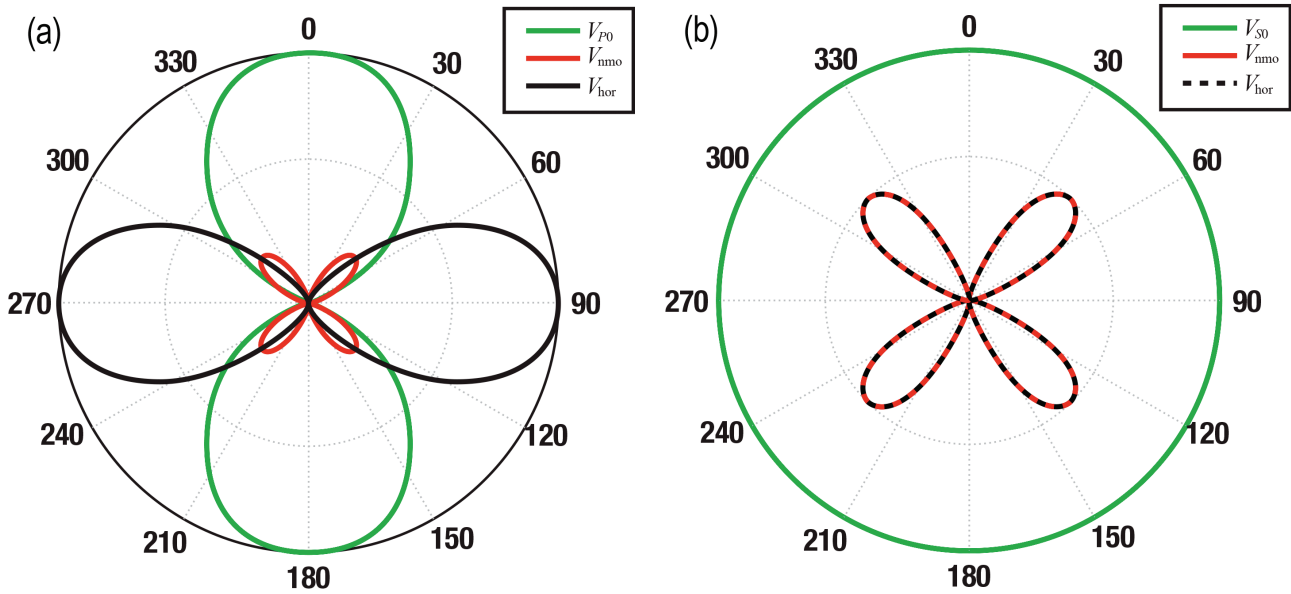


Figure 7 Radiation patterns of the transmitted (a) P-wavefield and (b) SV-wavefield. The perturbations in the velocities V_{p0} , V_{s0} , V_{nmo} , and V_{hor} are inserted into an isotropic homogeneous background. The patterns here are plotted in terms of incidence angle.

elastic model is sensitive to V_{s0} (Figure 8a) and could provide constraints for estimating the shear-wave vertical velocity.

It is clear from the P-wave radiation patterns that there is almost no trade-off between V_{p0} and V_{hor} . However, because an anomaly in V_{hor} mostly scatters energy at large opening angles (Figure 8a), the vertical wavenumbers for the inverted V_{hor} should be much lower than those for V_{p0} (Wu and Toksöz, 1987).

The radiation patterns of the SV-wave reflection for the velocities V_{nmo} and V_{hor} are close to those for transmitted SV-waves. The scattered energy for an anomaly in V_{s0} is no

longer distributed uniformly, but has maxima at incidence angles of 0° , 45° , and 90° (Figure 8b).

P-wave radiation patterns for the velocities V_{p0} , V_{nmo} and V_{hor} are generally close for elastic and acoustic media. The pattern for V_{nmo} in Figure 8 is different from the pattern in Figure 6 because here we use parameterization in terms of velocities and represent the patterns as functions of the incidence angle. However, it should be emphasised that in elastic media, P-waves can be used to constrain the velocity V_{s0} ; also, we may be able to obtain additional information about V_{p0} , V_{nmo} and V_{hor} from SV-wave data.

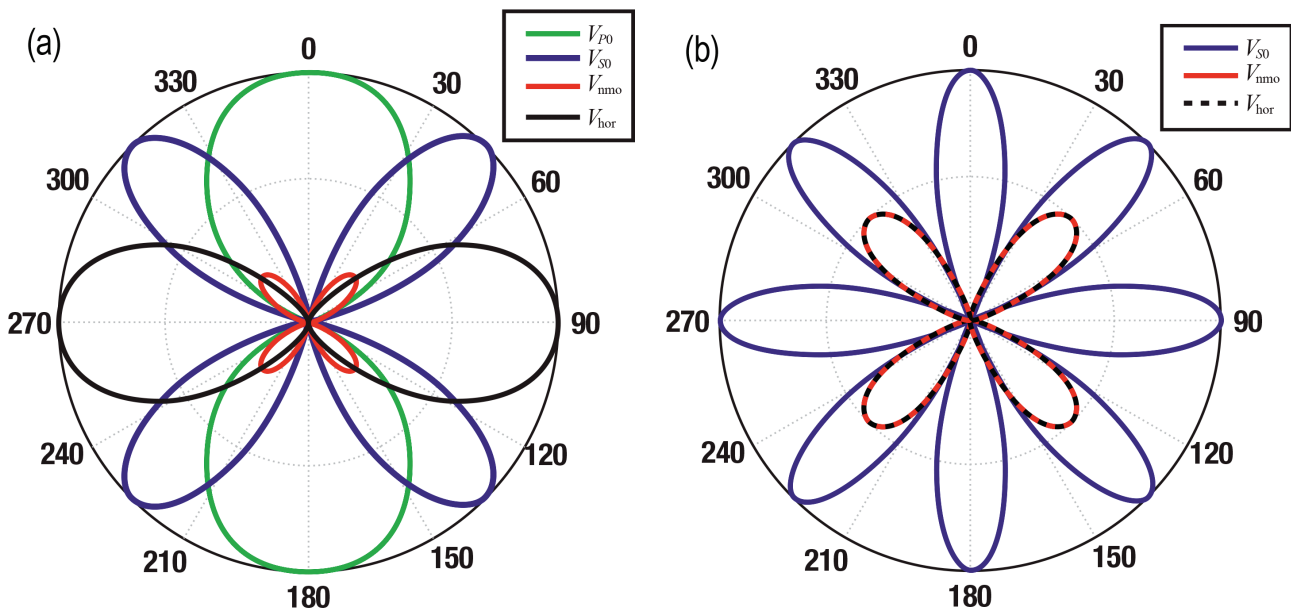


Figure 8 Radiation patterns for the reflected (a) P-wavefield and (b) SV-wavefield. The perturbations in V_{p0} , V_{s0} , V_{nmo} , and V_{hor} are inserted into an isotropic homogeneous background. The patterns here are plotted in terms of incidence angle.

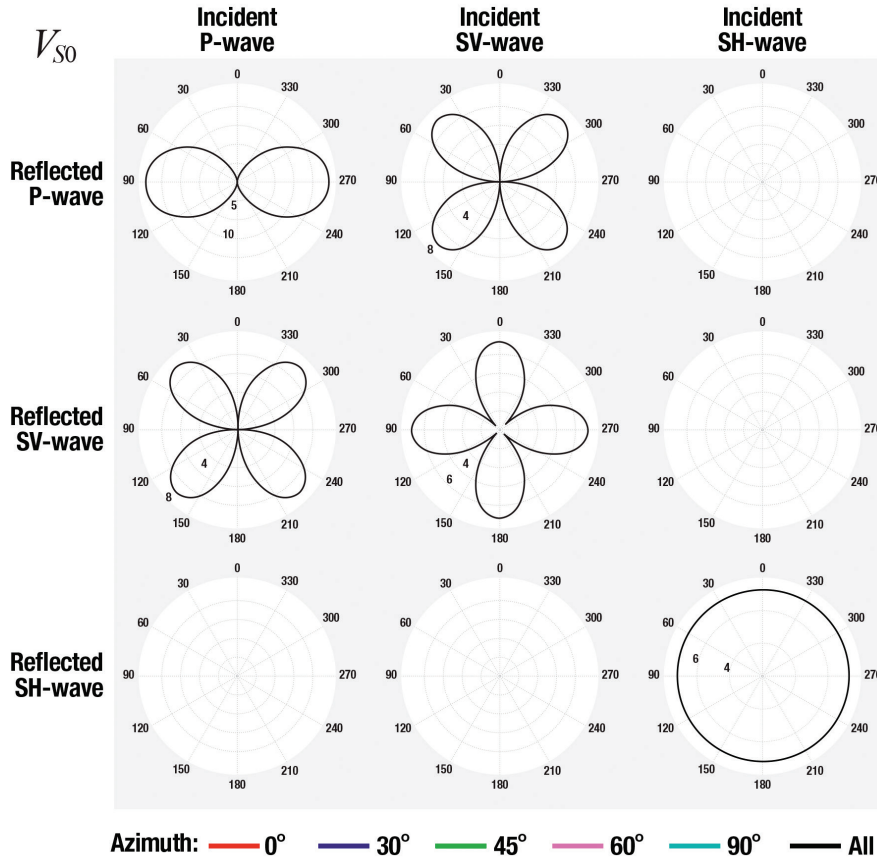


Figure 9 Radiation patterns for a perturbation in V_{S0} corresponding to different combinations of wave modes reflected from a horizontal interface. The employed parameterisation eliminates the azimuthal dependence of the radiation patterns, so that colours corresponding to different azimuths overlap. The numbers on the polar co-ordinates (or on the contours) describe the relative scattering magnitude.

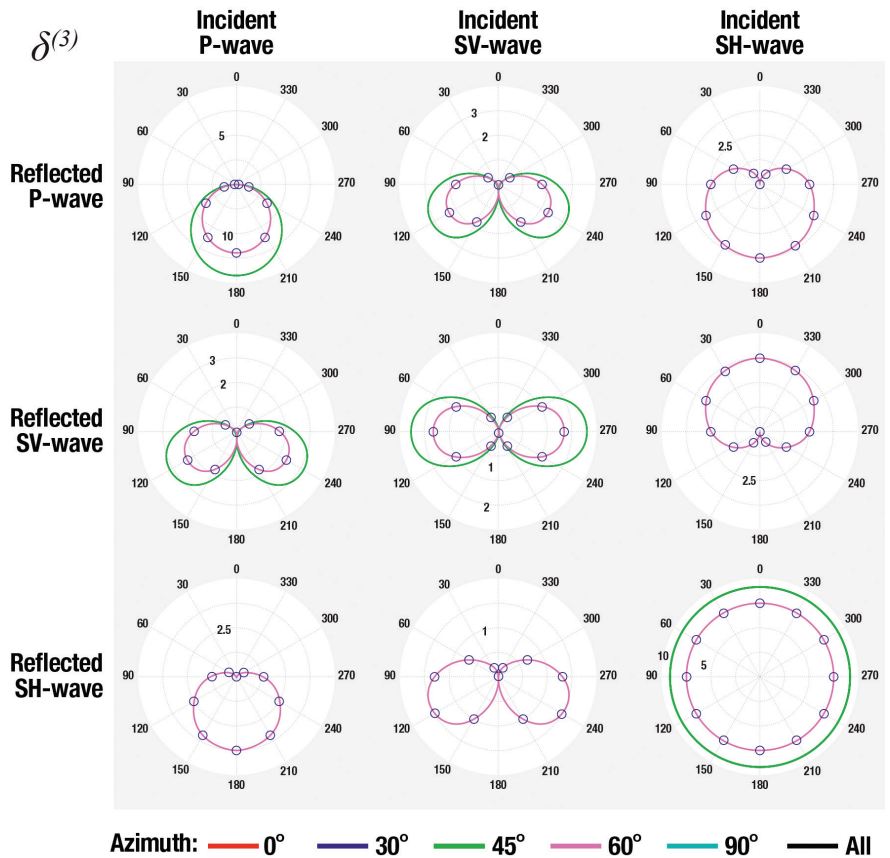


Figure 10 Radiation patterns for a perturbation in $\delta^{(3)}$ corresponding to different combinations of wave modes reflected from a horizontal interface. In this case, the patterns vary with azimuth. The missing colours imply zero scattering.

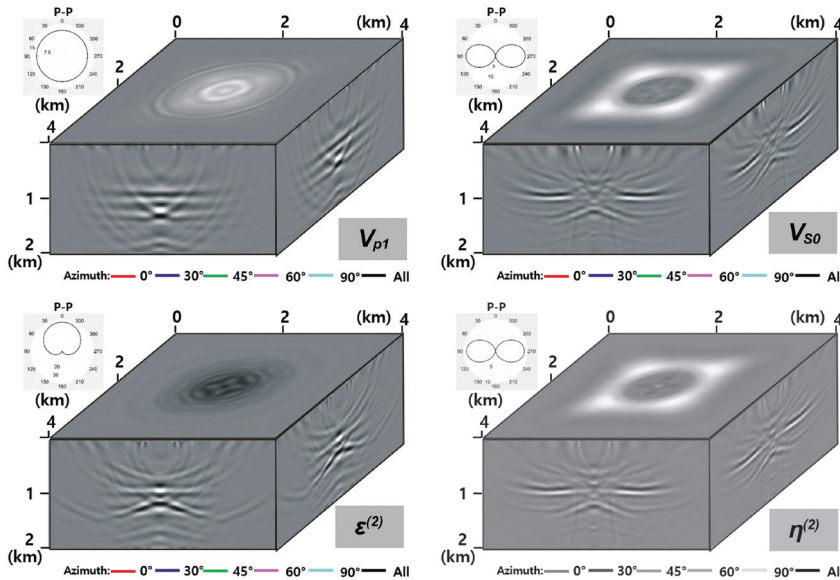


Figure 11 High-resolution FWI gradients for some of the parameters of orthorhombic media. The gradients correspond to P-wave scattering for a model with a horizontal reflector at 1 km; the source is located at the surface in the middle of the model, and receivers cover the entire surface. Also plotted are the radiation patterns corresponding to the incident and reflected P-waves. The background is isotropic with the velocity of the first layer. With this parameterization, the parameters have no azimuthal variation.

Elastic orthorhombic media

Development of elastic orthorhombic FWI is a big but doable task. The complexity lies in the computational cost and the potentially large null space for the inversion of surface seismic (even multi-component) data. Regularization and other assumptions can reduce the null space, but they may introduce bias in the results owing to incorrect a priori information. A well-designed parameterization, which can mitigate the potential negative impact of regularization, is extremely important for such complex models as orthorhombic given the immense computational cost of FWI. Through analysis of parameterization at various wavelength scales and of parameter sensitivity for the transmission, diffraction, and reflection data components, one can achieve a clear understanding of the resolution and accuracy of a selected parameter set. Because the optimal parameter set can also be tied to reservoir attributes such as fracture density and fluid content (using certain rock-physics relationships), the inversion can be tailored to update those parameters more rigorously. This also means that some other reservoir attributes might not be resolvable at the desired scale from surface seismic data, but at least we would know that in advance.

Figures 9 and 10 show examples of the radiation patterns for various wave-mode combinations. We consider a parameterization that includes V_{s0} , V_{p1} ($V_{p1} = V_{p0} \sqrt{1 + 2\epsilon^{(2)}}$ is the P-wave velocity in the x_1 -direction) and seven dimensionless parameters corresponding to the velocity ratios with respect to V_{s0} and V_{p1} . In other words, V_{s0} and V_{p1} become the reference velocity parameters, while the rest of the coefficients describe the anisotropic angular variation. In the case of a perturbation in V_{p1} , for an incident P-wave the scattered energy represents a P-wave with a purely isotropic response in scattering angle or azimuth (not shown here to save space). This response is identical to the one for the reference velocity in isotropic and VTI media with the same parameterization (e.g., see Figure 6). On the other hand, a perturbation in V_{s0}

(Figure 9) causes P-wave scattering from an incident P-wave, as well as mode conversions into the vertical shear (SV) waves. It does not, however, generate any mode conversions between the shear waves because the perturbation is in one of the vertical shear-wave velocities. Another observation is that the radiation patterns depend on the scattering angle, but not azimuth, so they are similar to patterns in elastic VTI media.

Finally, for a perturbation in $\delta^{(3)}$, which is equivalent to Thomsen’s δ in the $[x_1, x_2]$ plane, the radiation pattern does depend on azimuth (Figure 10). This example illustrates the possibility to formulate a parameterization that allows us to move from isotropic to VTI to elastic orthorhombic media with the same radiation patterns for the parameters shared by these models (for instance, the radiation pattern for the horizontal velocity V_{p1} is the same for VTI and orthorhombic media). This should help us to extend FWI from an initial isotropic model to orthorhombic media in a seamless manner.

The most important and time-consuming part of an FWI code is the extrapolation engine. Solving the elastic wave equation would result in a 4D wavefield in time and space, often simulated using a staggered-grid finite-difference (SGFD) extrapolator, which can be regarded as a mature modelling technique for orthorhombic media. In the next section, we discuss the possibility of implementing a spectral scheme based on wave-mode decomposition for FWI.

As a test, we compute the FWI gradients with the SGFD extrapolator and compare them with the radiation patterns discussed earlier. The gradients are calculated with the adjoint-state method by cross-correlating the source wavefield with the adjoint wavefield from the data (the cross-correlation weights depend on the scattering angle). To condition the gradient, we use a Limited-memory Broyden–Fletcher–Goldfarb–Shanno (LBFGS) algorithm.

The model in Figure 11 includes a horizontal reflector at 1 km depth, with perturbations in the model parameters embedded in an isotropic background. Using this background

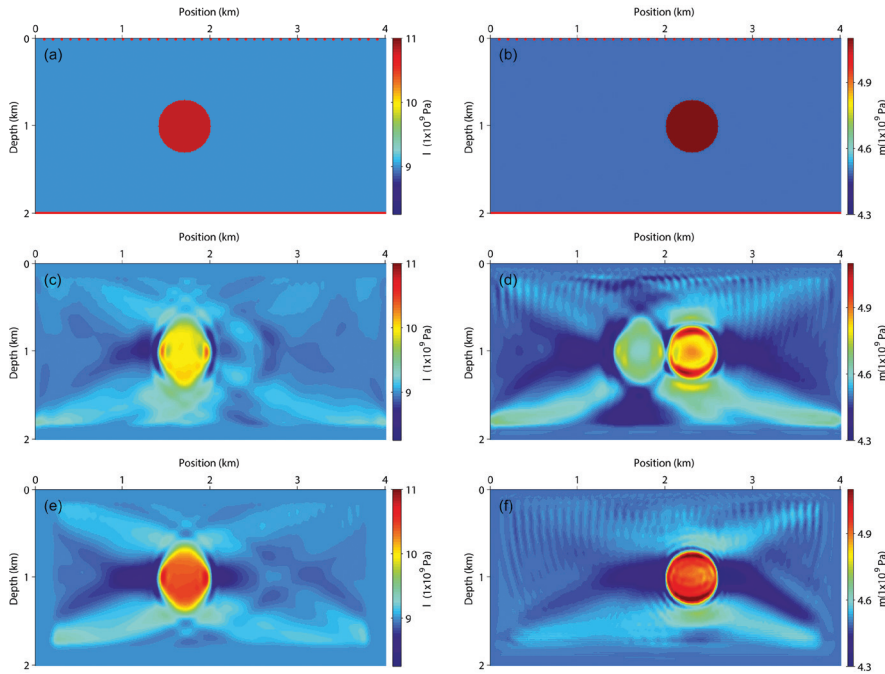


Figure 12 Elastic FWI of transmission data for models with anomalies in the Lamé parameters (a) λ and (b) μ at different locations in a homogeneous constant-density isotropic background. Inverted models using conventional (c and d) and mode-decomposition-based (e and f) FWI.

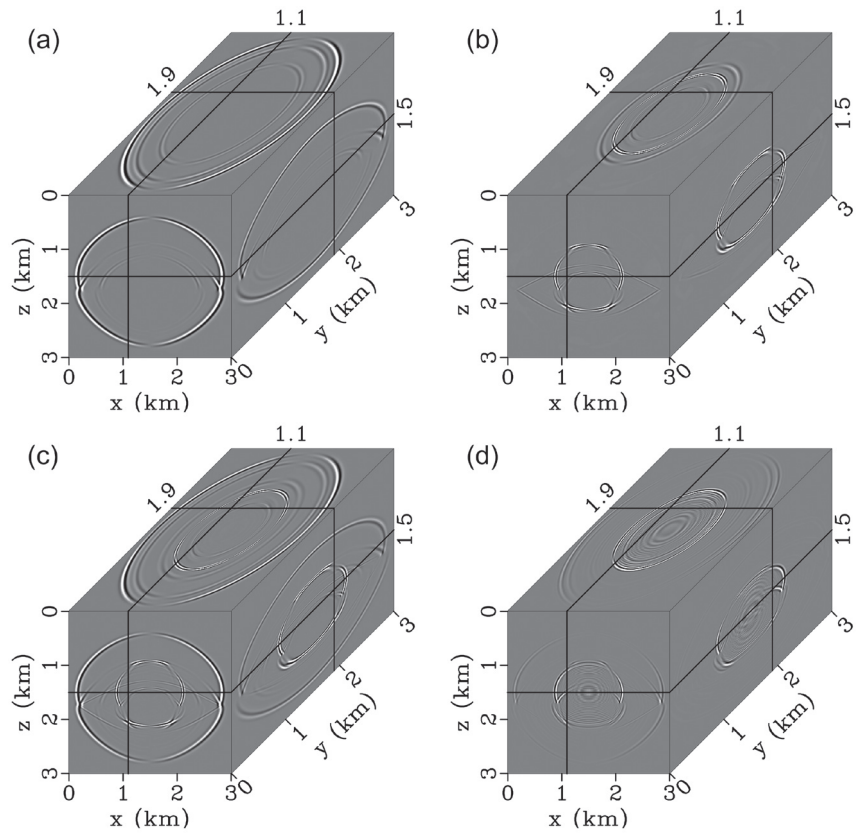


Figure 13 Decomposed (a) P- and (b) S-wavefields and (c) the total displacement fields for a two-layer model in which the first layer is VTI and the second is 'standard' orthorhombic. An explosive source is located at the centre of the model. (d) The total displacement field synthesized by using the 10th-order FD scheme. Only the x-component of displacement is shown to save space.

model, we predict data corresponding to a shot at the surface in the middle of the survey; owing to the homogeneity of the background model only the direct arrivals will match those recorded by the receivers at the surface. Of course, with the constant initial velocity, we are unable to predict the reflections. For this shot, we compute the gradients cor-

responding to the model parameters and show four of them in Figure 11 for P-wave reflection data.

In particular, for the P-wave velocity in the x_1 -direction, the gradient resembles an image of the reflector. The amplitude looks evenly distributed, as expected from the isotropic nature of the corresponding radiation pattern. On

the other hand, the perturbation in the shear-wave vertical velocity does not produce short-offset reflections, which is evident from both the gradient and the radiation pattern. The same observation can be made for the $\eta^{(2)}$ -perturbation. Note that the gradient for the parameter $\epsilon^{(2)}$, which is close to fractional difference between the P-wave velocity in the x_1 - and x_3 -directions, is in agreement with its radiation pattern, in which most energy is focused at zero offset.

Modelling (towards understanding the practicality)

Wave-mode decomposition for FWI

Seismic wave propagation is governed by P- and S-wave velocities, density, anisotropy parameters and attenuation (the latter is not discussed in this paper but represents a topic of ongoing research). As mentioned above, because of trade-offs it is difficult if not impossible to update all medium parameters. Generally, multi-parameter inversion needs multi-stage strategies, in which one would successively operate with different parameter classes and/or on different subsets of seismic data. Recently, Wang and Cheng (2015) suggested mitigating trade-offs through wave-mode decomposition, which aims to address the overlap of Fréchet-derivative wavefields during gradient calculation. As shown in Figure 12, the conventional conjugate-gradient method suffers from the cross-talk problem, while preconditioning of the gradients through wave-mode decomposition substantially improves the performance of gradient-based inversion. For isotropic media, this kind of preconditioning involves almost no extra computational cost. However, wave-mode decomposition in anisotropic media is expensive because the required operators are velocity-dependent and, therefore, not stationary. As demonstrated by Cheng and Fomel (2014), wave-mode decoupling can be achieved using a Fourier integral operator of the general form in a mixed domain (namely, the space-wavenumber domain). When combining wavefield extrapolation and mode decoupling for preconditioning the gradients, a spectral scheme based on the Fourier transform (instead of the FD method) is used. This overcomes numerical dispersion at higher frequencies, which hampers FD modelling.

Cheng et al. (2016) have developed an efficient spectral modelling approach based on low-rank decomposition of the mixed-domain integral operators to directly extrapolate the decoupled elastic displacement fields. Figure 13 shows displacement fields synthesized using the proposed approach in a ‘standard’ orthorhombic model representing a vertically fractured VTI layer (Schoenberg and Helbig, 1997; Tsvankin, 1997) above a horizontal reflector. Compared with the 10th-order FD scheme using the same spatial and temporal grids, the new spectral method is more efficient in simulating dispersion-free elastic wave propagation for both the decomposed and total displacement fields. This modelling engine allows us to extend elastic FWI based on mode decomposition from isotropic to TI and orthorhombic models.

The discussion in the previous two sections is focused on addressing the physics correctly, which involves making the

model azimuthally anisotropic, and on applying radiation pattern analysis to identify the parameters we can effectively invert for. These results give us a better chance of estimating reservoir properties with high resolution and reasonable computational speed using the new modelling algorithms described in this section (e.g., wave-mode decomposition). Given the complexity of the problem, it may be necessary to carry out target-oriented inversion, where only the reservoir itself is orthorhombic. In many cases, we should be able to treat the overburden as transversely isotropic and use less demanding inversion algorithms to account for its influence.

Conclusions

We briefly reviewed the shortcomings of the ‘classic’ seismic reservoir characterization workflows, as well as the important lessons we have learnt from them. The difficulty of replacing the current practice is obvious, and we argued that any new, more advanced alternative should incorporate the best features of the existing methods. Along these lines, we aspire to develop an FWI-based approach to reservoir characterization which would potentially change the way we currently work. As an example, migration will disappear from the existing workflows because the reservoir parameters will be estimated directly from recorded gathers. Although practical applications may be some years away, it is an objective that is well worth pursuing. The proposed methodology does require multi-disciplinary skills, and our strategy involves including many lessons learnt so far in different disciplines. Some examples are the inclusion of rock-physics constraints, the role of facies, orthorhombic anisotropy, efficient spectral modelling and analysis of radiation patterns. Of course, we have not covered many other components of the method, such as accounting for attenuation, but our aim is to address those as we progress in our research.

With efficient forward modelling and the parameterization optimized through sensitivity analysis, we may be able to invert for some reservoir attributes such as fracture parameters and facies under certain assumptions. Sensitivity analysis is particularly important because the success of our strategy will depend on the signature of each parameter in multi-azimuth and, possibly, multi-component recorded data. The resolution of the inverted parameters will be controlled by the behaviour of their scattering potential, the illumination provided by the data, and the frequency bandwidth.

Acknowledgements

This publication is based on work supported by the King Abdullah University of Science and Technology (KAUST) Office of Sponsored Research (OSR) under Award No 2230. The authors acknowledge partial support from the Consortium on Seismic Inverse Methods for Complex Structures at the Center for Wave Phenomena, Colorado School of Mines. The authors would also like to thank Ikon Science for its participation in this project and Patrick Corbett and the anonymous reviewers for improving the clarity of the paper.

References

- Alkhalifah, T. and Tsvankin, I. [1995]. Velocity analysis for transversely isotropic media. *Geophysics*, **60**, 1550-1566.
- Alkhalifah, T. and Plessix, R. [2014]. A recipe for practical full-waveform inversion in anisotropic media: An analytical parameter resolution study. *Geophysics*, **79**, R91-R101.
- Alkhalifah, T. [2015]. Conditioning the full waveform inversion gradient to welcome anisotropy. *Geophysics*, **80**, R111-R122.
- Calvet, M., Chevrot, S. and Souriau, A. [2006]. P-wave propagation in transversely isotropic media: I. Finite-frequency theory. *Physics of the Earth and Planetary Interiors*, **156**, 12–20.
- Cheng, J.B. and Fomel, S. [2014]. Fast algorithms of elastic wave mode separation and vector decomposition using low-rank approximation for anisotropic media. *Geophysics*, **79**, C97–C110.
- Cheng, J.B., Alkhalifah, T., Wu, Z.D., Zou, P. and Wang, C.L. [2016]. Simulating propagation of decoupled elastic waves using low-rank approximate mixed-domain integral operators for anisotropic media. *Geophysics*, **81**, T63-T77.
- Cohen, J. and Bleistein, N. [1977]. Seismic waveform modelling in a 3D earth using the born approximation: potential shortcomings and a remedy. *J. Appl. Math*, **32**, 784–799.
- Coléou, T., Allo, F., Bornard, R., Hamman, J. and Caldwell, D. [2005]. Petrophysical seismic inversion. *75th SEG annual meeting*, Expanded Abstracts, 1355-1358.
- Dellinger, J. and Etgen, J. [1990]. Wavefield separation in two-dimensional anisotropic media. *Geophysics*, **55**, 914–919.
- Gholami, Y., Brossier, R., Operto, S., Ribodetti, A. and Virieux, J. [2013]. Which parameterisation is suitable for acoustic vertical transverse isotropic full waveform inversion? Part 1: Sensitivity and trade-off analysis. *Geophysics*, **78**, R81–R105.
- Grechka, V. and Kachanov, M. [2006]. Effective elasticity of fractured rocks: A snapshot of the work in progress. *Geophysics*, **71**, W45-W58.
- Guasch, L., Warner, M., Nangoo, T., Morgan, J., Umpleby, A., Stekl, I. and Shah, N. [2012]. Elastic 3D full-waveform inversion. *82nd SEG Annual International Meeting*, Expanded Abstracts.
- Kamath, N. and Tsvankin, I. [2014]. Sensitivity analysis for elastic full-waveform inversion in VTI media. *84th SEG Annual International Meeting*, Expanded Abstracts.
- Kemper, M., and Gunning, J. [2014]. Joint impedance and facies inversion – seismic inversion redefined. *First Break*, **32**, 89-95.
- Operto, S., Gholami, Y., Prioux, V., Ribodetti, A., Brossier, R., Metivier, L. and Virieux, J. [2013]. A guided tour of multiparameter full-waveform inversion with multicomponent data: From theory to practice. *The Leading Edge*, **32**, 1040-1054.
- Panning, M., Capdeville, Y. and Romanowicz, A. [2009]. An inverse method for determining small variations in propagation speed. *Geophys. J. Int.*, **177**, 161–178.
- Psaila, D. [2011]. Stochastic Inversion of Pre-Stack Seismic Data into Geological Modelling Grids. *EAGE/SPE Joint Workshop-Closing the Loop*, Extended Abstracts, A02.
- Russell, B.H. [1988]. *Introduction to seismic inversion methods*. Society of Exploration Geophysicists.
- Saussus, D. and Sams, M. [2012]. Facies as the key to using seismic inversion for modelling reservoir properties. *First Break*, **30**, 45-52.
- Schoenberg, M. and Helbig, K. [1997]. Orthorhombic media: Modeling elastic wave behavior in a vertically fractured earth. *Geophysics*, **62**, 1954–1974.
- Shen, X. [2012]. Early-arrival waveform inversion for near-surface velocity and anisotropic parameter: Parametrization study. *82nd SEG Annual International Meeting*, Expanded Abstracts.
- Song, X. and Alkhalifah, T. [2013]. Modeling of pseudo-acoustic P-waves in orthorhombic media with lowrank approximation. *Geophysics*, **78**, C33-C40.
- Thomsen, L. [1986]. Weak elastic anisotropy. *Geophysics*, **51**, 1954-1966.
- Tsvankin, I. [1997]. Anisotropic parameters and P-wave velocity for orthorhombic media. *Geophysics*, **62**, 1292-1309.
- Tsvankin, I. [2012]. *Seismic signatures and analysis of reflection data in anisotropic media*, 3rd edition. Society of Exploration Geophysicists.
- Tsvankin, I. and Grechka, V. [2011]. *Seismology of azimuthally anisotropic media and seismic fracture characterization*. Society of Exploration Geophysicists.
- Vavryčuk, V. [2007]. Asymptotic Green's function in homogeneous anisotropic viscoelastic media. *Proceedings of the Royal Society A. Mathematical, Physical and Engineering Science*, **463**, 2689–2707.
- Wang, T.F. and Cheng, J.B. [2015]. Elastic wave mode decoupling for full waveform inversion. *85th SEG Annual International Meeting*, Expanded Abstracts.
- Wu, R. and Toksöz, M. [1987]. Diffraction tomography and multisource holography applied to seismic imaging. *Geophysics*, **52**, 11–25.
- Yan, J. and Sava, P. [2008]. Isotropic angle domain elastic reverse time migration. *Geophysics*, **73**, S229–S239.

Received: 21 December 2015; Accepted: 5 September 2016
Doi:10.3997/1365-2397.2016015



Geomodel-2017

11-14 September 2017 - Gelendzhik, Russia

Call for Abstracts deadline:
20 May 2017